COMMUNICATION

# Stereostructural Analysis of Flexible Oxidized Fatty Acids by VCD Spectroscopy

Tohru Taniguchi,*[a] Naka Ida,[b] Takuya Kitahara,[b] Davidson Obinna Agbo[b] and Kenji Monde*[a]

Received 00th January 20xx,
Accepted 00th January 20xx

DOI: 10.1039/x0xx00000x

**Oxidation of polyunsaturated fatty acids produces various oxidized lipids whose absolute configuration (AC) and conformations are difficult to analyze due to their flexibility. Through studies on hydroxy fatty acids, lipid hydroperoxides, and lipid epoxides, this work demonstrates the effectiveness of VCD spectroscopy to elucidate their AC and conformational preferences.**

Polyunsaturated fatty acids (PUFAs) and their esters are essential components of cell membranes and regulate the functions of various biomolecules. These lipids are susceptible to oxidative stress and are transformed to myriad oxidized molecular species. Enzymatic oxidation of PUFAs (*e.g.*, transformation of arachidonic acid to leukotrienes) produces a series of signalling molecules in animal as well as plant kingdoms.[1] Non-enzymatic lipid oxidation by reactive oxygen species has less been studied, but recent studies revealed that autoxidized lipids display significant biological activities that include induction of ferroptosis, a new type of regulated cell death.[2] Introduction of a single oxygen atom yields lipid epoxides and hydroxy fatty acids, whereas two atoms of oxygen results in lipid hydroperoxides. These modifications introduce one or more chiral centers to the lipids, but their absolute configuration (AC) has rarely been studied in relation to their biological activities, especially for autoxidized lipids. Moreover, seldom studied are conformational outcomes by lipid oxidation, which are of interest for development of bioactive analogues of oxidized lipids as drug candidates.[3] Development of a method that provides deeper insight into their structures should advance the fields of lipid biochemistry and medicinal chemistry.

Due to the extreme flexibility, fatty acids represent one of the most challenging molecular classes for structural elucidation. Flexible molecules are less likely to form fine crystals suitable for X-ray crystallography. While crystalline sponge method[4] and the cryoEM method microED[5] are emerging revolutionary methods for structural elucidation, their applicability to highly flexible molecules are yet to be studied. The AC of hydroxy fatty acids may be determined by installation of a chiral auxiliary group and the following NMR analysis (*e.g.*, Mosher-Kusumi method).[6] Alternatively, when authentic molecules are available (*e.g.*, by total synthesis), comparison of retention time on chiral HPLC column could elucidate the AC of the lipids of interest upon optimization of separation and detection conditions.[7] While these methods are useful for AC assignment, a method that informs both AC and conformation without the need of chemical derivatization and authentic samples is more desired.

Vibrational circular dichroism (VCD) spectroscopy has proven effective for AC and conformation analysis of various molecules. This technique relies on the comparison of experimental spectrum and theoretical one, whose calculations necessitate identification of all the stable conformers. Because of this requirement, VCD analysis has been best applied to rigid molecules.[8] Another difficulty for VCD studies of flexible molecules is their lower VCD intensities than those typically observed for rigid ones. Nevertheless, Merten *et al.* demonstrated that flexible hydroxyl diterpenes exhibited detectable VCD signals and assigned their ACs with using thorough theoretical calculations.[9] However, application of VCD spectroscopy to oxidized fatty acids, which are characteristic in their unbranched hydrocarbon structures, has not been reported. In continuation of our VCD studies on lipids,[10] this work demonstrates that VCD technique elucidates the AC and conformational features of hydroxy fatty acids, lipid hydroperoxides, and lipid epoxides. To test the feasibility of VCD structural analysis of oxidized lipids, those readily obtained in large amounts were studied here (Scheme 1). Note that it is not the goal of this work to establish a microgram-scale analysis

[a] *Frontier Research Center for Advanced Material and Life Science, Faculty of Advanced Life Science, Hokkaido University, Kita 21 Nishi 11, Sapporo 001-0021, Japan*
[b] *Graduate School of Life Science, Hokkaido University, Kita 21 Nishi 11, Sapporo 001-0021, Japan*

Electronic Supplementary Information (ESI) available. Figures S1-8 and Tables S1 and S2; Experimental and computational details; synthesis and characterization of **3**-**8**, **12**, and **14**; Cartesian coordinates of selected conformers. See DOI: 10.1039/x0xx00000x

method for biologically minuscule oxidized lipids (*e.g.*, prostaglandins). To our knowledge, this is the first report for the application of VCD spectroscopy to the AC assignment of fatty acids and of naturally occurring hydroperoxides.

We started with VCD studies on ricinoleic acid (**1**). Hydroxy $C_{18}$ fatty acid **1** normally exists as a triglyceride ricinolein (**2**, a main component of castor oil) and is a selective agonist for prostaglandin $EP_3$ receptor,[11] a protein targeted by clinically used medicines.[3a, 3c] Compound **1** was dissolved in $CDCl_3$ at a concentration of 0.6 M and its VCD spectrum was measured. Despite its high flexibility, the unbranched fatty acid **1** exhibited several characteristic VCD signals in the 1500-1000 $cm^{-1}$ region (Fig. 1a). See Fig. S1 for the IR spectra of the studied molecules in the 1900-1000 $cm^{-1}$ region.

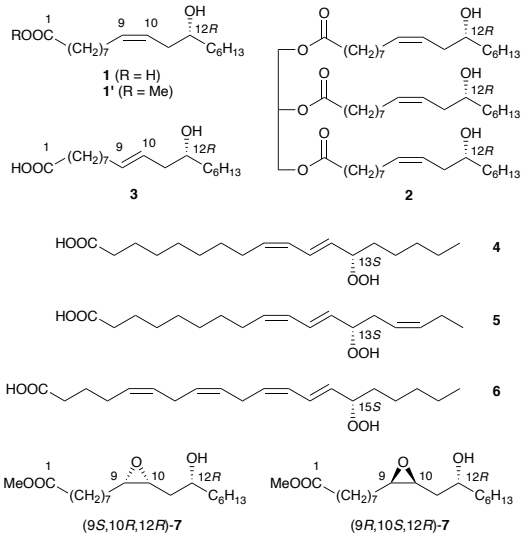


**Scheme 1** Structures of chiral oxidized lipids studied in this work: ricinoleic acid (**1**), methyl ricinoleate (**1′**), ricinolein (**2**), ricinelaidic acid (**3**), 13-HpODE (**4**), 13-HpOTE (**5**), 15-HpETE (**6**), and methyl 9,10-epoxy-12-hydroxyoctadecanoate (**7**).

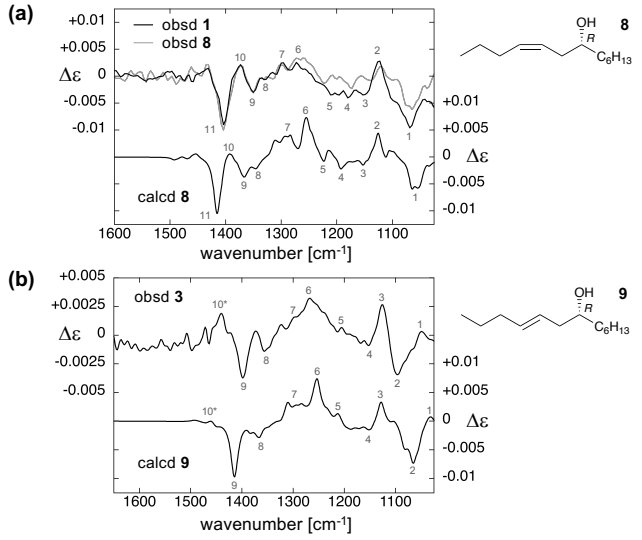


**Fig. 1** Comparison of the experimental and theoretical VCD spectra of hydroxy fatty acids and their truncated models. (a) VCD spectra of **1** and **8**. (b) VCD spectra of **3** and **9**. Corresponding VCD peaks are labelled, while nonmatching peaks are indicated by asterisks. Measurement conditions: 0.6 M in $CDCl_3$; $l$ = 85 μm. Calculation conditions: DFT/B3LYP/6-311+G(d,p)/PCM (chloroform). Scaling factor: 0.99.

Theoretical VCD calculations of the whole structure of **1** was difficult because of its numerous possible conformational states. Assuming the structure around the C12 chiral center to be the main source of the VCD signals, we designed a truncated $C_{13}$ model **8** for calculations. Suitability of **8** for interpreting the VCD spectrum of **1** was supported by their closely similar experimental spectra (Fig. 1a). Especially, these VCD spectra in the region above 1300 $cm^{-1}$, including the negative peak at 1404 $cm^{-1}$, were almost superimposable. See ESI for the synthesis of **8**.

Calculations of **8** started with a MMFF conformational search using a Monte Carlo algorithm, which led to more than 160 conformers within 3.0 kcal/mol from the most stable. These MMFF conformers were optimized at the DFT/B3LYP/6-31G(d) level of theory. The resultant 38 conformers in a 2.0 kcal/mol energy window were further optimized using B3LYP/6-311+G(d,p) with PCM for chloroform, leading to 19 conformers within 1.60 kcal/mol from the most stable. The latter energy window was set to consider all the conformers with a Boltzmann distribution of more than 1.0% for the following VCD calculations. VCD spectra of these conformers were calculated at the same level of theory and the final spectrum was obtained by weighted-average of the predicted spectra for each conformer based on its Boltzmann population. See Table S1a for the conformers of **8** considered for VCD calculations. Theoretical IR spectra of truncated models are shown in Fig. S1.

Major VCD signals observed for **1** showed a one-to-one correspondence to the calculated ones for **8** (Fig. 1a), including the 1404 $cm^{-1}$ negative band attributed to O-H and C-H deformations at the chiral center. Quantitative assessment of their similarity using CompareVOA software also led to a 99% confidence level for *R* stereochemistry (Table S2).[12] From these results, the oxidized fatty acid **1** can be assigned as *R* without prior knowledge on its AC. Calculation of a shorter $C_9$ model indicated that consideration of two $C_4$ unbranched hydrocarbon chains attached to the chiral center may be satisfactory for AC assignment in the case of **1** (Fig S2), although consideration of longer chains should increase the reliability of AC and conformational analysis. Theoretical VCD spectra of **8** calculated using other conditions are also shown in Fig S2.

Local conformation of **1** was also analyzed through studies on **8**. Dihedral angles around the chiral center of predicted conformers of **8** are listed in Table S1a. Each of these conformers exhibited different VCD patterns; for example, the negative signal at around 1404 $cm^{-1}$ was absent for some conformers (Fig. S3). None of each conformer presented VCD spectra that well reproduced the experimental spectrum of **1**. Thus, the obtained agreement between the population-weighted final spectrum and the experimental one suggested the accuracy of the prediction of the local conformational preferences. These results revealed the effectiveness of VCD spectroscopy for conformational analysis of oxidized lipids. Conformational features of **1** around the hydroxy chiral center seem largely maintained in acyl ester **1′** and triglyceride **2**, as all of these lipids showed similar VCD patterns (Fig. S4).

The structure of ricinelaidic acid (**3**), the C=C stereochemical isomer of **1**, was also studied in a similar manner (Fig. 1b). The

 

VCD spectrum calculated for a $C_{13}$ model **9** showed a good agreement with that observed for **3** (see Table S2 for qualitative analysis), with which its AC and local conformation were determined (Table. S1b). Note that the assignment of C=C double bond geometry in these molecules by VCD spectroscopy may not be practical because of the close similarity between the calculated VCD spectrum of **8** and that of **9** (see Fig. S5 for their direct comparison).

Studies on **1** and **3** demonstrated the capability of VCD spectroscopy to elucidate the structures of hydroxy fatty acids whose chiral center has a β,γ-unsaturated alkyl chain and a saturated alkyl chain. Oxidation of PUFAs often starts with production of lipid hydroperoxides whose chiral center is connected to an α,β-unsaturated hydrocarbon chain and either a β,γ-unsaturated or fully saturated hydrocarbon chain. To examine the applicability of VCD spectroscopy to flexible lipid hydroperoxides, we then studied naturally-occurring bioactive 13-HpODE (**4**), 13-HpOTE (**5**), and 15-HpETE (**6**). More than 50 mg each of these lipids were prepared starting from the corresponding PUFAs by enzymatic oxidation using soybean lipoxygenase, which selectively produces *S* enantiomers.[13] The resultant lipid hydroperoxides were dissolved in $CDCl_3$ and their VCD spectra were scanned at an ambient temperature for 1 hour. These molecules showed weak but detectable VCD signals (Fig. 2a and 2b). All of **4**-**6** showed a negative VCD band at ca 1330 $cm^{-1}$ and a positive one at ca 1350 $cm^{-1}$. No decomposition was detected by NMR spectroscopy of the recovered samples after VCD measurement (data not shown). The VCD spectra of **4** and **6** showed similar signal patterns, which is reasonable considering their identical local structures.

In a similar manner to the design and calculations of **8**, truncated models **10** (a fragment of **4** and **6**) and **11** (a fragment of **5**) were used for VCD calculations. Theoretical VCD spectra of both **10** and **11** predicted signals at ca 1330 $cm^{-1}$ and ca 1350 $cm^{-1}$ with the correct sign (Fig. 2a and 2b). Based on analysis of these vibrational modes, we ascribed the former signal to a O-H deformation and the latter primarily to a C-H deformation at the asymmetric carbon (Fig. S6). The agreement between the observed and calculated signals led to the determination of their ACs as *S* configuration. See Table S2 for the quantitative comparison. While a VCD study of a synthetic tertiary alkyl hydroperoxide was reported,[14] the current work is the first to apply VCD spectroscopy to naturally-occurring hydroperoxides.

Conformational features of secondary alkyl hydroperoxides have rarely been studied. We thus studied the local conformations of the hydrocarbon backbone and the OOH functional group of **4**-**6**. Conformational analysis of models **10** and **11** found their local conformational preferences such as dihedral angles ϕ (C4-C5-C6-C7) of ca -130° and ξ (C5-C6-O1-O2) of ca -70° (Fig. 2c and 2d and Table S1c and S1d). VCD calculations of conformational sets with different values of ϕ and ξ resulted in totally different spectral patterns (Fig. S7). These results not only suggested that the characteristic VCD signals at around 1330 and 1350 $cm^{-1}$ are highly sensitive to the local conformations but also bolstered the accuracy of the predicted conformational preferences.

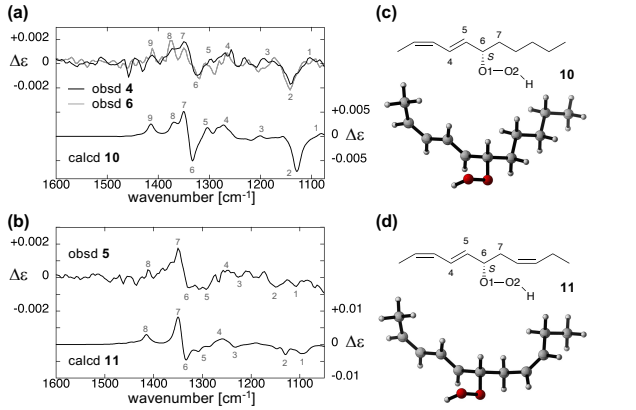


**Fig. 2** Comparison of the experimental and theoretical VCD spectra of lipid hydroperoxides and their truncated models. (a) VCD spectra of **4**, **6**, and **10**. (b) VCD spectra of **5** and **11**. Corresponding VCD peaks are labelled. (c) Chemical structure of **10** and the most stable predicted conformer. (d) Chemical structure of **11** and the most stable predicted conformer. Measurement conditions: 1.5 M (for **4** and **6**) or 1.7 M (for **5**) in $CDCl_3$; *l* = 85 μm. Calculation conditions: DFT/B3LYP/6-311+G(d,p)/PCM (chloroform). Scaling factor: 0.98.

The effectiveness of VCD spectroscopy to structural analysis of oxidized lipids demonstrated so far is realized by its high sensitivity to distinguish two hydrocarbon chains with slightly different unsaturation patterns attached to the chiral centers. In fact, methyl (*R*)-12-hydroxyoctadecanoate (**12**), a saturated hydroxy fatty acid ester obtained by hydrogenation of **1′**, showed an almost flat VCD spectrum (Fig S4). Thus, although VCD spectroscopy is generally applicable to unsaturated oxidized lipids originating from PUFAs, its utility to saturated hydroxy fatty acids and fatty acid esters of hydroxy fatty acids (*i.e.*, FAHFAs)[15] should be examined in a future study.

Last, we applied VCD spectroscopy to a pair of lipid epoxide diastereomers **7**. Biological generation of lipid hydroperoxides is often followed by their transformation to lipid epoxides (*e.g.*, conversion of 5-HpETE to leukotriene $A_4$). Lipid epoxides have also been chemically prepared as useful synthetic intermediates for functionalization of unsaturated lipids.[16] See references for applications of VCD spectroscopy to other epoxide-containing natural products.[17]

A diastereomer of **7a** with δ 3.90 ppm for H-12 was obtained by stereoselective epoxidation of **1′** using $VO(acac)_2$ and the following silica-gel column chromatography purification.[18] The other diastereomer **7b** with δ 3.84 ppm (H-12) was obtained starting from **1′** by benzoylation, oxidation using *m*CPBA, diastereoseparation on chiral HPLC column, and the following removal of the benzoyl group. These diastereomers showed readily distinguishable VCD patterns (Fig. 3): **7a** displayed a negative band at 1414 $cm^{-1}$, while **7b** displayed a positive-negative-positive pattern (1124, 1140, and 1157 $cm^{-1}$).

VCD calculations were performed for fragments (5*S*,6*R*,8*R*)-**13** and (5*R*,6*S*,8*R*)-**13**. Among several calculation conditions tested, M06-2X/6-311+G(d,p)/PCM (chloroform) provided VCD spectra well reproducing the observed spectral features. The calculated VCD spectrum of (5*S*,6*R*,8*R*)-**13** exhibited a similar pattern to that observed for **7a** such as a negative signal at 1414 $cm^{-1}$ (Fig. 3a). Meanwhile, the theoretical one for (5*R*,6*S*,8*R*)-**13** presented a similar positive-negative-positive pattern (1122,

1143, and 1173 $cm^{-1}$) to that observed for **7b**, with the predicted positive signal at 1173 $cm^{-1}$ being weaker than that observed at 1157 $cm^{-1}$ (Fig. 3b). Such qualitative visual inspection as well as quantitative comparison (Table S2) reliably assigned the AC of **7a** and **7b** as 9*S*,10*R*,12*R* and 9*R*,10*S*,12*R*, respectively. These assignments were bolstered by a 2-step conversion of **7a** to a 10,12-acetonide (**14**) and the following nOe measurement (Fig. S8). These results confirmed that the stereostructure of lipid epoxides can also be elucidated by VCD spectroscopy.

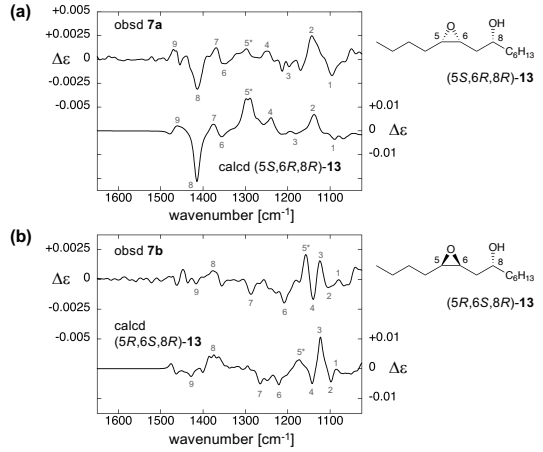


**Fig. 3** Comparison of the experimental and theoretical VCD spectra of lipid epoxides and their truncated models. (a) VCD spectra of **7a** and (5*S*,6*R*,8*R*)-**13**. (b) VCD spectra of **7b** and (5*R*,6*S*,8*R*)-**13**. Corresponding VCD peaks are labelled, while nonmatching peaks are indicated by asterisks. Measurement conditions: 1.1 M (for **7a**) or 2.2 M (for **7b**) in $CDCl_3$; *l* = 100 μm (for **7a**) or 50 μm (for **7b**). Calculation conditions: DFT/M06-2X/6-311+G(d,p)/PCM (chloroform). Scaling factor: 0.97.

In summary, this paper reports the first application of VCD spectroscopy to chiral fatty acids and to naturally-occurring hydroperoxides. The studied lipids exhibited weak VCD signals probably due to the flexibility of their overall structures and subtle structural differences between two hydrocarbon chains attached to the chiral center. Nevertheless, we demonstrated that, with using suitable models for VCD calculations, the AC and conformational preferences of unsaturated hydroxy fatty acids, lipid hydroperoxides, and lipid epoxides can be reliably elucidated. This work also identified characteristic VCD signals sensitive to the conformation of lipid hydroperoxides. As the AC and conformation of lipids are important for their biological functions, we hope that the insight brought by VCD spectroscopy be used for future lipid biochemistry and development of lipid-related medicines. Further VCD studies on functionalized oxidized lipids will be reported in due course.

The authors thank the Instrumental Analysis Division, Global Facility Center, Creative Research Institution, Hokkaido University, for NMR and HRMS measurements. This work was supported by KAKENHI Grant No. JP26702034, JP18H02093, and JP19H02836.

## Notes and references

1. (a) J. Z. Haeggström and C. D. Funk, *Chemical Reviews*, 2011, **111**, 5866-5898; (b) C. A. Rouzer and L. J. Marnett, *Chemical Reviews*, 2011, **111**, 5899-5921.
2. (a) U. Jahn, J.-M. Galano and T. Durand, *Angew. Chem. Int. Ed.*, 2008, **47**, 5894-5955; (b) H. Yin, L. Xu and N. A. Porter, *Chem. Rev.*, 2011, **111**, 5944-5972; (c) S. J. Dixon, K. M. Lemberg, M. R. Lamprecht, R. Skouta, E. M. Zaitsev, C. E. Gleason, D. N. Patel, A. J. Bauer, A. M. Cantley, W. S. Yang, B. Morrison and B. R. Stockwell, *Cell*, 2012, **149**, 1060-1072.
3. (a) T. Hirata and S. Narumiya, *Chem. Rev.* 2011, **111**, 6209-6230; (b) M. Nakamura and T. Shimizu, *Chem. Rev.*, 2011, **111**, 6231-6298; (c) J. J. Moreno, *Eur. J. Pharmacol.*, 2017, **796**, 7-19.
4. Y. Inokuma, S. Yoshioka, J. Ariyoshi, T. Arai, Y. Hitora, K. Takada, S. Matsunaga, K. Rissanen and M. Fujita, *Nature*, 2013, **495**, 461-466.
5. (a) T. Gruene, J. T. C. Wennmacher, C. Zaubitzer, J. J. Holstein, J. Heidler, A. Fecteau-Lefebvre, S. De Carlo, E. Müller, K. N. Goldie, I. Regeni, T. Li, G. Santiso-Quinones, G. Steinfeld, S. Handschin, E. van Genderen, J. A. van Bokhoven, G. H. Clever and R. Pantelic, *Angew. Chem. Int. Ed.*, 2018, **57**, 16313-16317; (b) C. G. Jones, M. W. Martynowycz, J. Hattne, T. J. Fulton, B. M. Stoltz, J. A. Rodriguez, H. M. Nelson and T. Gonen, *ACS Cent. Sci.*, 2018, **4**, 1587-1592.
6. I. Ohtani, T. Kusumi, Y. Kashman and H. Kakisawa, *Journal of the American Chemical Society*, 1991, **113**, 4092-4096.
7. M. Blum, I. Dogan, M. Karber, M. Rothe and W.-H. Schunck, *Journal of Lipid Research*, 2019, **60**, 135-148.
8. (a) Y. He, B. Wang, R. K. Dukor and L. A. Nafie, *Appl. Spectrosc.*, 2011, **65**, 699-723; (b) J. M. Batista, E. W. Blanch and V. D. Bolzani, *Nat. Prod. Rep.*, 2015, **32**, 1280-1302; (c) A. Mándi and T. Kurtán, *Nat. Prod. Rep.*, 2019, **36**, 889-918; (d) C. Merten, T. P. Golub and N. M. Kreienborg, *J. Org. Chem.*, 2019, **84**, 8797-8814; (e) P. L. Polavarapu and E. Santoro, *Nat. Prod. Rep.*, 2020, **37**, 1661-1699.
9. (a) C. Merten, V. Smyrniotopoulos and D. Tasdemir, *Chem. Commun.*, 2015, **51**, 16217-16220; (b) V. Smyrniotopoulos, C. Merten, M. Kaiser and D. Tasdemir, *Marine Drugs*, 2017, **15**, 245.
10. T. Taniguchi, D. Manai, M. Shibata, Y. Itabashi and K. Monde, *J. Am. Chem. Soc.*, 2015, **137**, 12191-12194.
11. S. Tunaru, T. F. Althoff, R. M. Nüsing, M. Diener and S. Offermanns, *Proc. Nat. Acad. Sci.*, 2012, **109**, 9179-9184.
12. E. Debie, E. De Gussem, R. K. Dukor, W. Herrebout, L. A. Nafie and P. Bultinck, *ChemPhysChem*, 2011, **12**, 1542-1549.
13. M. J. Knapp and J. P. Klinman, *Biochemistry*, 2003, **42**, 11466-11475.
14. A. Lattanzi, A. Scettri, R. Zanasi, F. J. Devlin and P. J. Stephens, *The Journal of Organic Chemistry*, 2010, **75**, 2179-2188.
15. (a) M. M. Yore, I. Syed, P. M. Moraes-Vieira, T. Zhang, M. A. Herman, E. A. Homan, R. T. Patel, J. Lee, S. Chen, O. D. Peroni, A. S. Dhaneshwar, A. Hammarstedt, U. Smith, T. E. McGraw, A. Saghatelian and B. B. Kahn, *Cell*, 2014, **159**, 318-332; (b) M. G. Kokotou, A. C. Kokotos, D. Gkikas, O. G. Mountanea, C. Mantzourani, A. Almutairi, X. Lei, S. Ramanadham, P. K. Politis and G. Kokotos, *J. Med. Chem.*, 2020, **63**, 12666-12681.
16. N. Funken, F. Mühlhaus and A. Gansäuer, *Angewandte Chemie International Edition*, 2016, **55**, 12030-12034.
17. (a) Y. Matsuo, S. Maeda, C. Ohba, H. Fukaya and Y. Mimaki, *Journal of Natural Products*, 2016, **79**, 2175-2180; (b) L. F. Julio, E. Burgueño-Tapia, C. E. Díaz, N. Pérez-Hernández, A. González-Coloma and P. Joseph-Nathan, *Chirality*, 2017, **29**, 716-725.
18. (a) E. D. Mihelich, K. Daniels and D. J. Eickhoff, *J. Am. Chem. Soc.*, 1981, **103**, 7690-7692; (b) M. N. B. Omar, R. J. Hamilton and H. A. Moynihan, *ARKIVOC*, 2003, **2003**, 190-199.

 